European Journal of Heart Failure (2010) **12**, 4–12
doi:10.1093/eurjhf/hfp165

MEF2 transcriptional activity maintains mitochondrial adaptation in cardiac pressure overload

Hamid el Azzouzi[1,2†], Ralph J. van Oort[2†], Roel van der Nagel[2], Wim Sluiter[3], Martin W. Bergmann[4], and Leon J. De Windt[1,2*]

[1]Department of Cardiology, Faculty of Health, Medicine and Life Sciences, Cardiovascular Research Institute Maastricht, Maastricht University, Maastricht, The Netherlands; [2]The Hubrecht Institute and Interuniversity Cardiology Institute Netherlands, Royal Netherlands Academy of Sciences, Utrecht, The Netherlands; [3]Departments of Neurology, Erasmus MC, Rotterdam, The Netherlands; and [4]Department of Cardiology, Charité-Universitätsmedizin Berlin, Franz Volhard Klinik, Max Delbrück Center for Molecular Medicine, Berlin, Germany

Received 18 December 2008; revised 11 August 2009; accepted 8 October 2009

Aims The transcription factor MEF2 is a downstream target for several hypertrophic signalling pathways in the heart, suggesting that MEF2 may act as a valuable therapeutic target in the treatment of heart failure.

Methods and results In this study, we investigated the potential benefits of overall MEF2 inhibition in a mouse model of chronic pressure overloading, by subjecting transgenic mice expressing a dominant negative form of MEF2 (DN-MEF2 Tg) in the heart, to transverse aortic constriction (TAC). Histological analysis revealed no major differences in cardiac remodelling between DN-MEF2 Tg and control mice after TAC. Surprisingly, echocardiographic analysis revealed that DN-MEF2 Tg mice had a decrease in cardiac function compared with control animals. Analysis of the mitochondrial respiratory chain showed that DN-MEF2 Tg mice displayed lower expression of NADH dehydrogenase subunit 6 (ND6), part of mitochondrial Complex I. The reduced expression of ND6 in DN-MEF2 Tg mice after pressure overload correlated with an increase in cell death secondary to overproduction of reactive oxygen species (ROS).

Conclusion Our data suggest that MEF2 transcriptional activity is required for mitochondrial function and its inhibition predisposes the heart to impaired mitochondrial function, overproduction of ROS, enhanced cell death, and cardiac dysfunction, following pressure overload.

Keywords MEF2 • NADH dehydrogenase subunit 6 • Transverse aortic constriction • Mitochondria • Heart failure • Reactive oxygen species

Introduction

In response to stress, the heart compensates by hypertrophic growth, which frequently progresses to cardiac dilation and heart failure. The initial hypertrophic response is associated with the activation of several intracellular signalling pathways.[1,2] These pathways are interconnected and culminate in the nucleus on only a few transcriptional regulators. With the hope of identifying novel therapeutic targets for the treatment of heart failure, much effort has been dedicated to dissecting the role of these select transcriptional factors. One common downstream transcriptional target for diverse stress cascades in the heart are members of the MEF2 family of MADS (*MCM1, agamous, deficiens, serum response factor*) box transcription factors.[3] The four vertebrate MEF2 factors, MEF2A, -B, -C, and -D, display overlapping expression patterns in embryonic and adult tissues.[4,5]

The normal adult heart exhibits only basal MEF2 transcriptional activity, which is likely required for the maintenance of expression of genes involved in cardiomyocyte homeostasis, maintenance of the contractile apparatus, and energy metabolism.[6,7] MEF2 activity is upregulated by prohypertrophic signalling cascade constituents, such as calcineurin, calcium/calmodulin-dependent protein kinase

†The first two authors contributed equally to the study.

* Corresponding author. Tel: +31 43 388 4307, Fax: +31 43 387 1055, Email: l.dewindt@maastrichtuniversity.nl

(CaMK), protein kinase C (PKC), protein kinase D, big mitogen-activated protein kinase (MAPK)-1 (BMK-1), and p38 MAPK.[6,8–10]

Despite the considerable amount of evidence suggesting that MEF2 factors promote hypertrophic cardiac growth, this hypothesis has only recently been tested in a more direct approach. We and others have shown that overexpression of MEF2A or MEF2C in the post-natal murine heart has minimal effects on cardiac growth but evokes features of dilated cardiomyopathy.[7,11–13] Conversely, *in vivo* inhibition of MEF2 activity resulted in minimal reduction of calcineurin induced hypertrophy, but prevented wall thinning and chamber dilation and significantly improved cardiac function.[12] Likewise, heart-restricted genetic deletion of the MEF2D isoform provided considerable protection against pressure overload-induced cardiac remodelling, dysfunction, and induction of foetal gene expression.[11] These results imply that MEF2 triggers the molecular and genetic factors underlying cardiac dilation and contractile loss, at least in certain experimental settings, which suggests that therapeutic MEF2 targeting may have potential for preventing chamber dilation and cardiac dysfunction in heart failure.

In this study, we directly tested the effects of MEF2 inhibition in cardiac hypertrophy and heart failure using a physiological model of pressure overload. To this end, conditional transgenic mice expressing a dominant-negative form of MEF2 (DN-MEF2) in the heart were subjected to transverse aortic constriction (TAC), a surgical model for pressure overload.

Methods

Mice

Details on the generation of transgenic mice conditionally expressing DN-MEF2 and mice expressing Cre recombinase under control of the 5.5 kb murine cardiac myosin heavy chain promoter (MHC-Cre) have been described in detail previously.[12,14]

Aortic banding

Transverse aortic constriction or sham surgery was performed in male mice, which were at least 10 weeks of age, by subjecting the aorta to a defined 27-gauge constriction between the first and second truncus of the aortic arch as described in detail previously.[15–17]

Transthoracic echocardiography

Five weeks after surgery, cardiac remodelling and function were assessed by non-invasive echocardiography using a VisualSonics Vevo 770 high-resolution imaging system equipped with a 30 MHz RMV-707B scanning head.[18] Echocardiographic measurements were performed on mice anaesthetized with isoflurane. In M-mode, the following parameters were obtained with three or more readings per mouse: left ventricular posterior wall thickness, interventricular septum thickness, end-diastolic left ventricular internal diameter, end-systolic left ventricular internal diameter, left ventricular fractional shortening (FS), and ejection fraction (EF). Fractional shortening was calculated as (LVIDd − LVIDs)/LVIDd × 100, echocardiographic LV mass (mg) was calculated by use of an uncorrected cube assumption as LV mass = $[(\mathrm{LVIDd} + \mathrm{LVPWd} + \mathrm{IVSd})^3 - (\mathrm{LVIDd})^3](1000)$, as described previously.[16] Doppler echocardiography was used to determine the pressure gradient between the proximal and distal sites of the TAC, and only mice with a pressure gradient >30 mmHg were used in this study.

Immunolabelling and histological analysis

Hearts were arrested in diastole and perfusion fixed with 4% paraformaldehyde and embedded in paraffin. Sections were stained with haematoxylin and eosin (H&E), Sirius red, or FITC-labelled wheat germ agglutinin (WGA-FITC) or incubated with an antibody against 8-OHdG (7.5 μg/μL; Oxis International Inc., Portland, Oregon). Envision+ Kit (Dako Cytomation, Glostrup, Denmark) was used as a secondary reagent. Staining was developed using DAB (brown precipitate), and slides counterstained with haematoxylin and visualized using a Nikon Eclipse E600 microscope (Nikon, Melville, New York, USA).[19]

Real-time RT–PCR RNA quantification

Total RNA was isolated from heart tissue using TRIzol reagent (Invitrogen, Carlsbad, CA, USA). One microgram of RNA was reverse transcribed using M-MLV reverse transcriptase (Promega, Madison, WI, USA). Real-time PCR using the Bio-Rad iCycler (Bio-Rad, Hercules, CA, USA) and fluorescence detection was performed in 96-well plates using SYBR Green and MyIQ optical software (Bio-Rad) as described in detail previously.[12] Primer sequences are available upon request.

Agilent gene expression profiling and data analysis

Total RNA was extracted using TRIzol (Invitrogen), cleaned with Qiagen RNAeasy Mini Kits (Qiagen), RNA quantity was measured with a NanoDrop® ND-1000 UV-Vis spectrophotometer (Wilmington), and RNA quality was monitored using an Agilent 2100 bioanalyser. Agilent 44K mouse whole genome microarray slides (Palo Alto) were used and a dye-swap experimental design applied. RNA samples (500 ng each) from three ventricles each of MHC-Cre and MHC-Cre/FloxDN-MEF2 mouse hearts were pooled, amplified, and labelled with Cy5- and Cy3-CTP (Perkin Elmer) to produce labelled cRNA using Agilent low RNA input fluorescent linear amplification kits following the manufacturers protocol. Dye–incorporation ratio was determined with a NanoDrop® ND-1000 UV-Vis spectrophotometer. For hybridization, the guidelines for 44K format arrays with cRNA targets were strictly followed. Briefly, 750 ng of Cy3-labelled cRNA and 750 ng Cy5-labelled cRNA were mixed and incubated with an Agilent microarray slide for 17 h using an Agilent *in situ* hybridization kit following SSC buffer washing. The washed slides were immediately dried, and scanned using Agilent DNA Microarray Scanner (G2565BA). Raw data were generated using Agilent's Feature Extraction software (FE v7.1). Data are presented in Supplementary material online, *Table S1*.

Western blot analysis

SDS–PAGE electrophoresis and blotting was performed as described in detail previously.[20] Antibodies used included a monoclonal OXPHOS Complexes cocktail (MitoSciences, 1:5000), polyclonal anti-PARP (Cell Signalling 1:500), and polyclonal anti-Cleaved PARP (Cell Signalling 1:500), followed by corresponding horseradish peroxidase-conjugated secondary antibodies (DAKO, 1:5000) and ECL detection.

Measurement of mitochondrial complex function

Procedures for isolation of mitochondria from snap-frozen hearts, citrate synthase activity, and Complex IV assays were performed as described previously.[16]

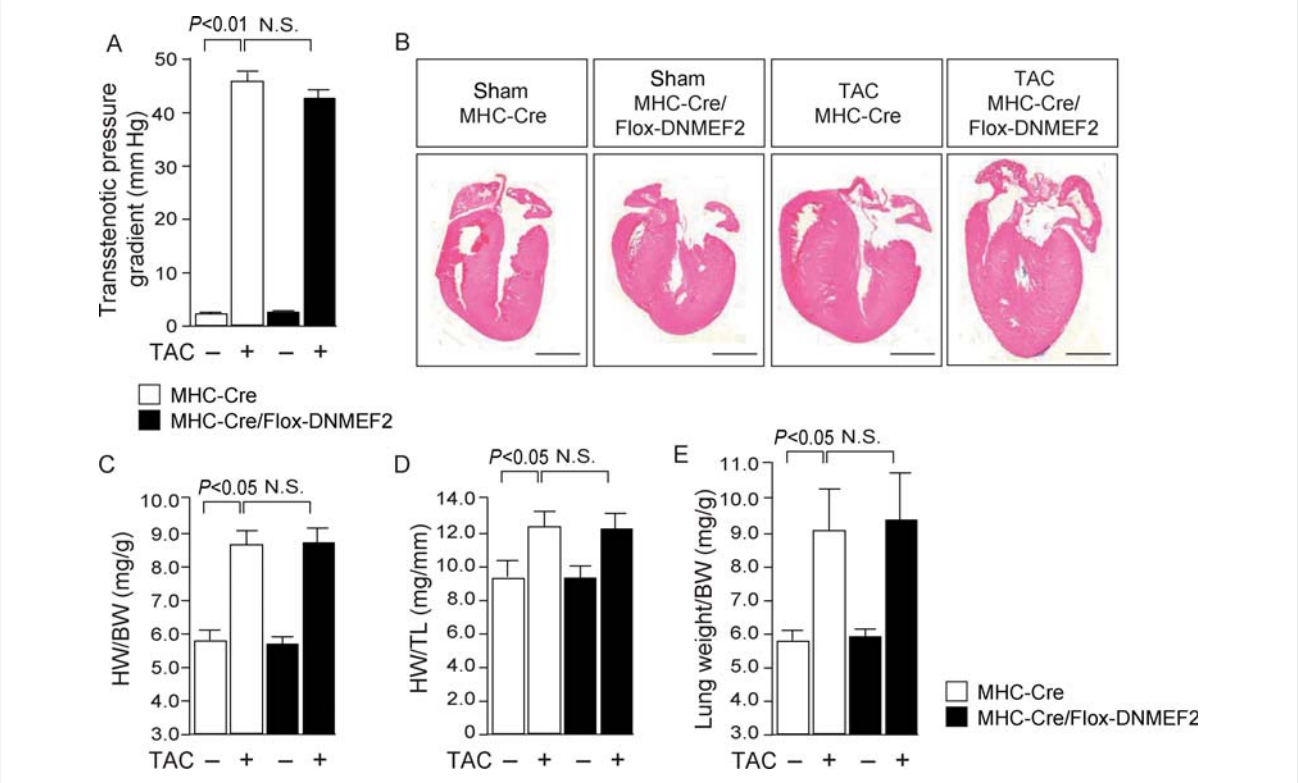

Figure 1 DN-MEF2 expression does not prevent pressure overload-induced cardiac hypertrophy. (*A*) Pressure gradients across the proximal and distal transverse aorta were measured invasively to validate the TAC procedure. (*B*) Representative gross morphology and H&E-stained four-chamber view of hearts dissected from 5-week-old mice of indicated genotypes, demonstrating a profound cardiac enlargement after pressure overload (bar 5 mm). (*C*) Heart weight to body weight (HW/BW) ratios, and (*D*) ratios of heart weight to tibia length (HW/TL) of the indicated groups show an equal hypertrophic response for MHC-Cre and MHC-Cre/FloxDN-MEF2 hearts 5 weeks after TAC ($n = 6$ per group). (*E*) Lung weight to body weight ratios indicate comparable increase in lung weight in both experimental groups after pressure overload ($n = 6$ per group). N.S., not significant.

TUNEL staining

TUNEL assays were performed as described previously,[16] using the *In Situ* Cell Death Detection TMR-Red Kit (Roche) and using an antibody against α-actinin (Sigma) and TO-PRO3 (Molecular Probes) on 10 μm frozen, apical cross-sections of hearts.

Statistical analysis

The results are presented as mean ± SEM. Statistical analyses were performed with InStat 3.0 (GraphPad Software, Inc., San Diego, CA, USA). The analyses consisted of ANOVA, followed by Tukey's post test when group differences were detected at the 5% significance level. Statistical significance was accepted at a *P*-value less than 0.05.

Results

Inhibition of MEF2 activity does not prevent pressure overload-induced cardiac hypertrophy

MEF2 transcription factors are activated by several intracellular hypertrophic signalling pathways.[1,2] Using transgenic mice that express a DN-MEF2 upon activation of Cre recombinase (FloxDN-MEF2 mice), we have recently demonstrated that inhibition of MEF2 transcriptional activity downstream of cardiac calcineurin signalling displayed a substantial reduction in cardiac dilation and improved contractility.[12] Accordingly, we used the same genetic loss-of-function approach to assess the role of MEF2 in pressure overload-induced cardiac remodelling, anticipating that heart-restricted MEF2 inhibition during pressure overload may also confer protection against this form of maladaptive remodelling.

To this end, we subjected MHC-Cre/FloxDN-MEF2 and control MHC-Cre mice to TAC or sham surgery, and analysed cardiac remodelling and function 5 weeks after surgery. The hypertrophic response in MHC-Cre/FloxDN-MEF2 mice after TAC was indistinguishable from that of pressure-overloaded MHC-Cre mice (*Figure 1A* and *B*). Heart weight-to-body weight (HW/BW) or heart weight-to-tibia length (HW/TL) ratios confirmed the increase in heart weight after pressure overload for both MHC-Cre and MHC-Cre/FloxDN-MEF2 mice compared with sham-operated mice (*Figure 1C* and *D*). Furthermore, pressure overload was associated with pulmonary oedema, as lung weight to body weight (LW/BW) increased to 7.2 ± 1.2 and 10.3 ± 1.8 (LW/BW) for MHC-Cre and MHC-Cre/FloxDN-MEF2 TAC mice (*Figure 1E*). The increase in these ratios for MHC-Cre/

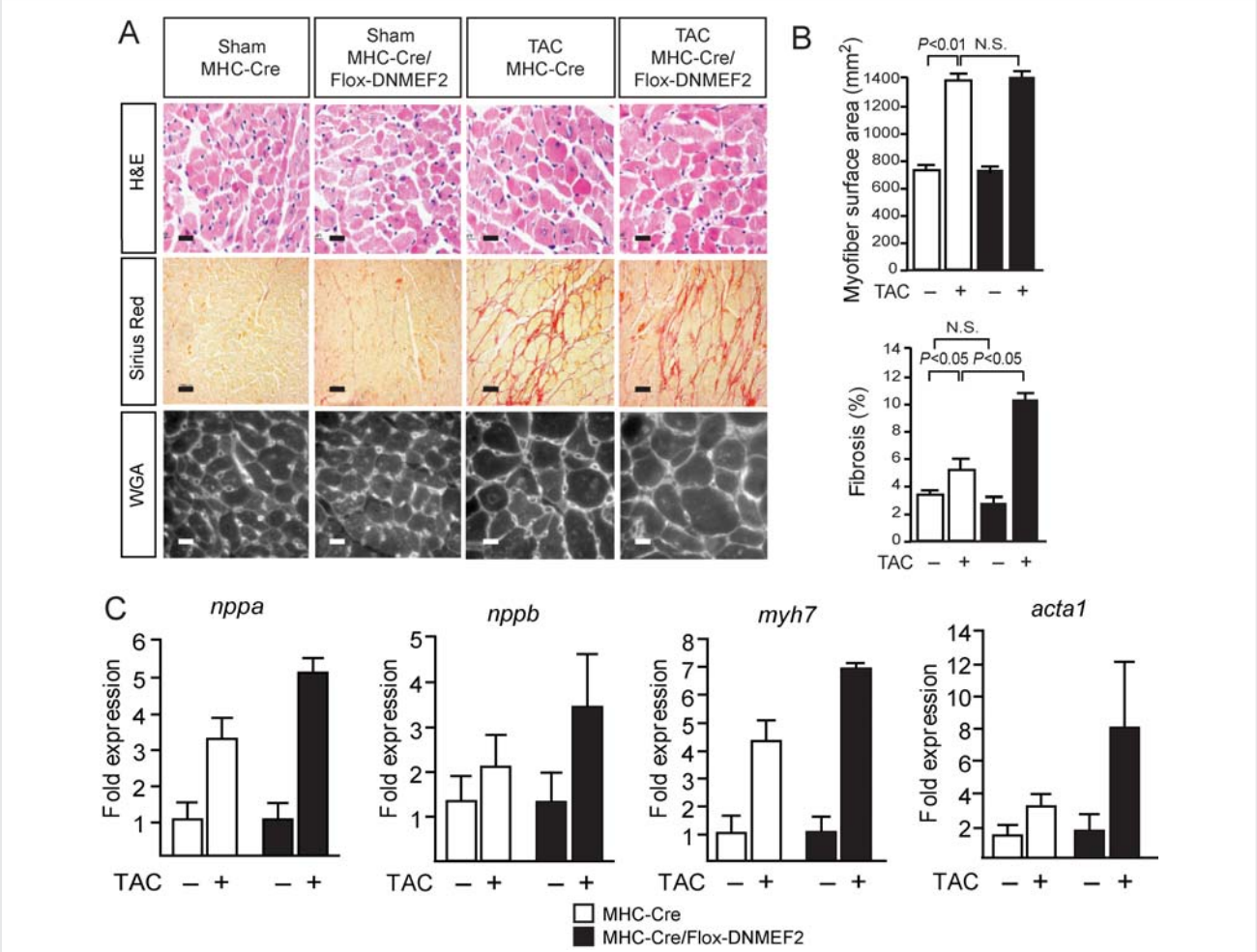

Figure 2 Gravimetric, histological, functional, and molecular analysis of MHC-Cre and MHC-Cre/FloxDN-MEF2 mice after TAC. (*A*) H&E-stained images reveal remarkable myocyte hypertrophy and myofibre disarray in MHC-Cre and MHC-Cre/FloxDN-MEF2 hearts subjected to pressure overload. Sirius red staining indicates massive interstitial and perivascular fibrosis in hearts from MHC-Cre and MHC-Cre/FloxDN-MEF2 mice subjected to pressure overload. Representative wheat germ agglutinin staining images of hearts from mice of indicated genotypes (bar 0.2 mm). (*B*) Quantification of myofibre cross-sectional area from indicated genotypes shows significant attenuation of myocyte hypertrophy in MHC-Cre and MHC-Cre/FloxDN-MEF2 mice subjected to pressure overload ($n = 3$ per group, with 100 fibres counted per animal). Quantification of fibrosis from indicated genotypes shows excessive deposition of fibrosis in MHC-Cre/FloxDN-MEF2 mice subjected to TAC ($n = 3$ per group). (*C*) Real-time PCR analysis for hypertrophic markers, all of which were increased to a similar extent in MHC-Cre and MHC-Cre/FloxDN-MEF2 mice subjected to pressure overload. N.S., not significant.

FloxDN-MEF2 TAC mice tended to be higher compared with those for MHC-Cre TAC mice (not significant), which may suggest that cardiac function after TAC was worsened in these mice. Thus, inhibition of MEF2 activity does not inhibit the hypertrophic response following pressure overload.

Haematoxylin and eosin- and Sirius red-stained cardiac histological sections did not show any signs of histopathology in sham-operated MHC-Cre/FloxDN-MEF2 and control MHC-Cre mice. In contrast, cardiomyocyte hypertrophy, myocyte disarray, and extensive areas of interstitial and perivascular fibrosis were evident in both pressure-overloaded MHC-Cre/FloxDN-MEF2 and MHC-Cre mice hearts (*Figure 2A*). As a more quantitative evaluation of individual myofibre hypertrophy, myofibril cross-sectional areas were quantified from WGA-stained sections. MHC-Cre/FloxDN-MEF2 and control MHC-Cre mice showed similar myofibre cross-sectional areas after TAC (*Figure 2B*). Quantification of fibrotic lesions demonstrated induction of fibrosis in control MHC-Cre mice after TAC, and a more pronounced deposition of fibrosis in MHC-Cre/FloxDN-MEF2 mice after TAC (*Figure 2B*).

Reactivation of foetal gene expression is a hallmark of pathological hypertrophy and heart failure, and therefore the expression levels of a number of foetal genes were determined. Transcripts for *nppa* (atrial natriuretic factor), *nppb* (brain natriuretic peptide), *myh7* (beta-MHC), and *acta1* (alpha-skeletal actin) were all strongly activated after TAC with no obvious difference between the two experimental groups (*Figure 2C*). Overall, our pressure overload regimen induced features of pathological cardiac remodelling, which seemed to worsen when MEF2 activity was genetically attenuated.

Table 1 Echocardiographic characteristics in MHC-Cre and MHC-Cre/FloxDN-MEF2 mice after sham operation and after transverse aortic constriction

	Sham		TAC	
	MHC-Cre	MHC-Cre/DN-MEF2	MHC-Cre	MHC-Cre/DN-MEF2
N	5	5	8	8
BW (g)	30.1 ± 3.8	33.8 ± 2.3	30.6 ± 2.2	25.6 ± 1.7
IVSs (mm)	1.13 ± 0.09	1.32 ± 0.08	1.41 ± 0.08	1.08 ± 0.05*
IVSd, (mm)	0.83 ± 0.06	0.92 ± 0.06	1.01 ± 0.05	0.84 ± 0.05
LVPWs (mm)	1.15 ± 0.09	1.21 ± 0.04	1.32 ± 0.05	1.10 ± 0.05*
LVPWd (mm)	0.75 ± 0.05	0.85 ± 0.02	0.98 ± 0.05†	0.87 ± 0.05
ESD (mm)	2.89 ± 0.15	2.60 ± 0.20	3.00 ± 0.29	3.44 ± 0.18*†
EDD (mm)	3.97 ± 0.13	3.82 ± 0.17	4.01 ± 0.24	4.16 ± 0.11
LV mass (mg)	119 ± 5	110 ± 11	162 ± 18†	146 ± 16†
FS (%)	27 ± 2	32 ± 3	27 ± 4	18 ± 3†
EF (%)	54 ± 4	61 ± 4	51 ± 6	37 ± 5†
AoPg (mmHg)	3 ± 1	3 ± 1	48 ± 3†	42 ± 2†

Data are expressed as mean ± SEM. AoPg, aortic pressure gradient; BW, body weight; EDD, end-diastolic diameter; EF, ejection fraction; ESD, end-systolic diameter; FS, left ventricular fractional shortening; IVS, intraventricular septal wall thickness; LVPW, left ventricular posterior wall thickness, TAC, transverse aortic constriction.
*$P < 0.05$ vs. MHC-Cre TAC.
†$P < 0.05$ vs. corresponding sham group.

Inhibition of MEF2 activity provokes exaggerated pressure overload-induced cardiac dysfunction

Heart geometry and function were also analysed by non-invasive echocardiography after TAC (*Table 1*). In agreement with the increased HW/BW and HW/TL ratios, thickening of the ventricular walls was evident in MHC-Cre mice, left ventricular posterior wall thickness at diastole (LVPWd) was 0.98 ± 0.05 mm for MHC-Cre TAC compared with 0.75 ± 0.05 mm for MHC-Cre sham mice ($P < 0.05$; *Table 1*). MHC-Cre/FloxDN-MEF2 mice, in contrast, displayed signs of wall thinning instead of thickening after induction of pressure overload. During systole, both intraventricular septal wall thickness (IVS) and LVPW were significantly decreased in MHC-Cre/FloxDN-MEF2 TAC mice (1.08 ± 0.05 and 1.10 ± 0.05 mm for IVSs and LVPWs, respectively) compared with MHC-Cre TAC mice (1.41 ± 0.08 and 1.32 ± 0.05 mm for IVSs and LVPWs, respectively, $P < 0.05$). Changes in heart geometry were accompanied by impaired cardiac function in MHC-Cre/FloxDN-MEF2 mice after TAC, as both FS and EF were significantly lower (18 ± 3 and 37 ± 5% for FS and EF, respectively) compared with MHC-Cre/FloxDN-MEF2 sham mice (32 ± 3 and 61 ± 4% for FS and EF, respectively; $P < 0.05$; *Table 1*).

Overall, these results indicate that inhibition of MEF2 activity does not prevent the development of cardiac hypertrophy and heart failure during pressure overload and suggest accelerated adverse adaptation to pressure overload.

Inhibition of MEF2 during pressure overload causes mitochondrial defects

The availability of energy in skeletal and cardiac muscle can be significantly altered in both health and disease. Chronic exercise in skeletal muscle, for example, stimulates a switching from predominantly glycolytic to more oxidative fibres, which contain more mitochondria and are resistant to fatigue.[21] Conversely, aberrations in energy production are seen in such diverse muscular diseases as muscular dystrophies, mitochondrial myopathies,[22] and chronic congestive heart failure.[23] Likewise, during pathological hypertrophy, mitochondrial adaptation is inadequate, which may be a contributing factor to cardiac decompensation.[23–25] As MEF2 is known to regulate the expression of genes involved in energy metabolism and of several nuclear encoded mitochondrial genes,[26] we hypothesized that the accelerated decompensation observed in pressure overloaded MHC-Cre/FloxDN-MEF2 mice may be related to impaired mitochondrial adaptation.

First, the level of mitochondrial matrix enzyme citrate synthase was determined as a reflection of the mitochondrial mass, to assess whether overall mitochondrial density was altered in MHC-Cre/FloxDN-MEF2 mice before or after pressure overload compared with MHC-Cre mice. No changes in mitochondrial density were detected among the experimental groups (*Figure 3A*). Next, we measured respiratory chain (RC) Complex IV activity in hearts from the experimental cohorts, which demonstrated that enzymatic activity of Complex IV was not different between MHC-Cre/FloxDN-MEF2 mice before or after pressure overload compared with MHC-Cre mice (*Figure 3B*). In contrast, using a mixture of monoclonal antibodies directed against various proteins in complexes of the electron transport chain, we found a specific decrease in expression of NADH dehydrogenase subunit 6 (ND6), part of mitochondrial complex 1, in MHC-Cre/FloxDN-MEF2 mice during pressure overload compared with MHC-Cre mice (*Figure 3C*). Real-time PCR analyses confirmed a significant decrease in ND6 transcript abundance in MHC-Cre/FloxDN-MEF2 compared with MHC-Cre after TAC (*Figure 3D*).

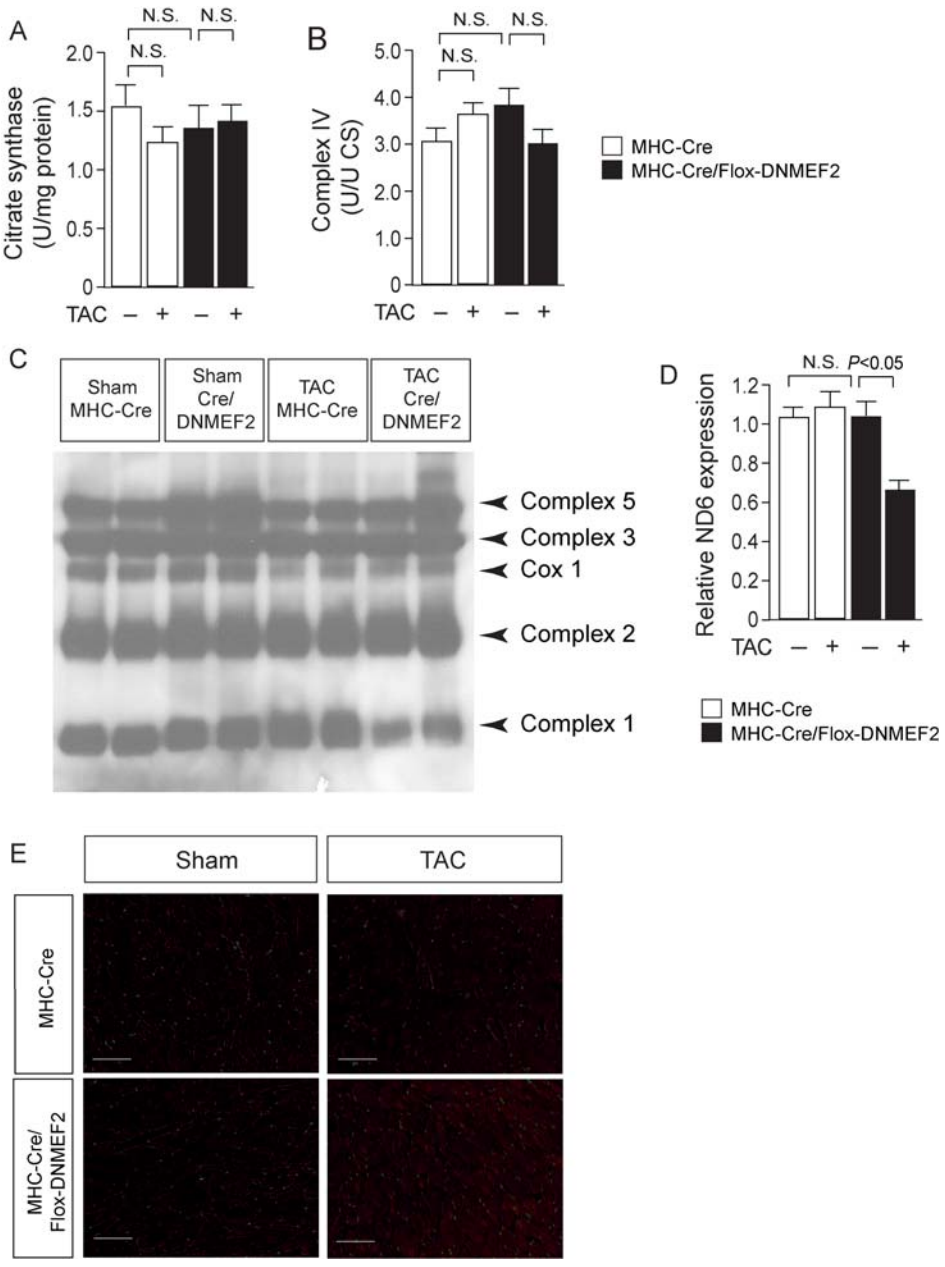

Figure 3 Inhibition of MEF2 during pressure overload causes mitochondrial defects. (*A*) Citrate synthase assays on hearts of 3-month-old MHC-Cre and MHC-Cre/FloxDN-MEF2 mice subjected to sham or TAC surgery indicate no differences in mitochondrial density between the experimental cohorts. (*B*) Measurement of respiratory chain Complex IV activity in cardiac mitochondria isolated from MHC-Cre and MHC-Cre/FloxDN-MEF2 mice demonstrated comparable Complex IV function. Complex IV activity values were standardized for the amount of mitochondria (citrate synthase). (*C*) Western blot analysis using a mixture of monoclonal antibodies directed against various proteins in complexes of the electron transport chain (ETC), showing decreased expression of NADH dehydrogenase subunit 6 (ND6). (*D*) Real-time PCR analysis confirmed a significant decrease in mRNA levels of ND6 in MHC-Cre/FloxDN-MEF2 compared with MHC-Cre after TAC. (*E*) Representative histological images of hearts of indicated genotypes (bar 0.2 mm) using 8-hydroxy-2′-deoxyguanosine (8-OHDG) as a marker for free radical DNA damage. Pressure overload elevated oxidative damage in both groups, with MHC-Cre/FloxDN-MEF2 mice displaying more oxidative damage than MHC-Cre after TAC. Sham-operated mice showed less 8-OHDG-positive nuclei. N.S., not significant.

Mutations in ND6 have been shown to result in Complex I dysfunction, provoking overproduction of reactive oxygen species (ROS).[27] To test whether the impaired expression of ND6 in pressure overloaded MHC-Cre/FloxDN-MEF2 mice may also cause excessive ROS production, we evaluated a downstream marker for oxidative stress related damage. The myocardium of al xperimental genotypes was stained for 8-hydroxy-2′-deoxyguanosine (8-OHDG), a marker for free radical DNA

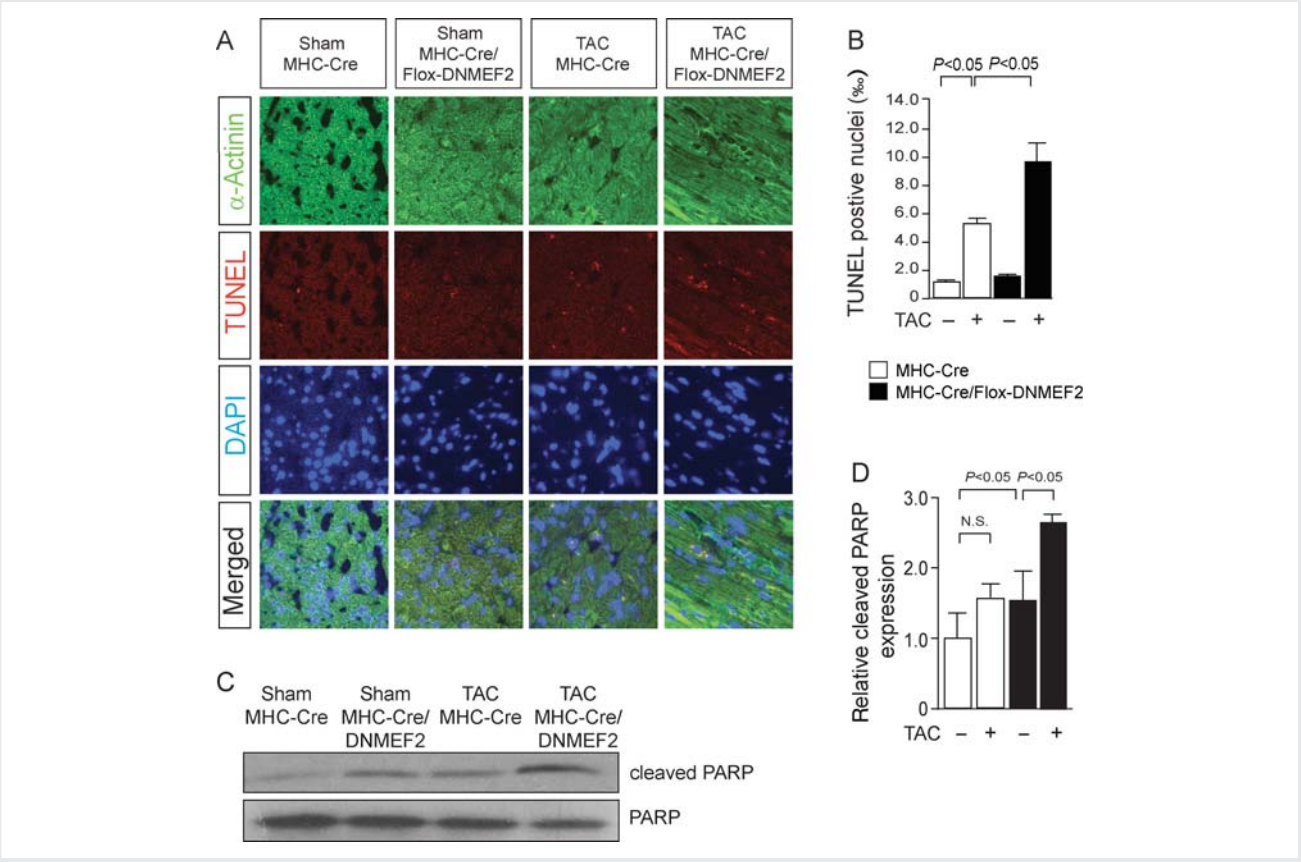

Figure 4 Inhibition of MEF2 results in ROS induced apoptosis during pressure overload. (*A*) Representative images of TUNEL labelling of myocardium of MHC-Cre and MHC-Cre/FloxDN-MEF2 mice 5 weeks after TAC or sham surgery. (*B*) Bar graph representation of the percentage of TUNEL positive cardiomyocytes in hearts of MHC-Cre and MHC-Cre/FloxDN-MEF2 mice subjected to sham or TAC surgery (1000 cells counted per animal, $n = 3$ per group), showing enhanced apoptosis in MHC-Cre/FloxDN-MEF2 hearts subjected to pressure overload. (*C*) Western blot showing increased cleaved PARP levels in MHC-Cre/FloxDN-MEF2 hearts subjected to pressure overload compared with pressure overloaded MHC-Cre hearts. (*D*) Quantification of cleaved PARP/total PARP as assessed by western blotting ($n = 3$). N.S., not significant.

damage. As expected, sham-operated mice showed a very low number of 8-OHDG-positive nuclei (*Figure 3E*). In contrast, pressure overload dramatically elevated the number of 8-OHDG-positive nuclei in both groups, with MHC-Cre/FloxDN-MEF2 mice displaying more evidence of nuclear oxidative damage than pressure-overloaded MHC-Cre mice (*Figure 3E*).

In summary, these data demonstrate that MHC-Cre/FloxDN-MEF2 mice at baseline have no signs of oxidative stress, like their control counterparts, but display excessive production of ROS and oxidative stress-induced damage following pressure overload.

Inhibition of MEF2 during pressure overload increases reactive oxygen species induced apoptosis in cardiomyocytes

Biomechanical stress activates signalling cascades,[28] predisposes cardiac muscle to late-onset apoptosis,[16,29–31] and provokes progressive left ventricular remodelling and heart failure.[29,30] Oxidative stress can become an additional physiological stressor for haemodynamically overloaded cardiomyocytes and can ultimately overwhelm protective cell survival pathways and result in apoptotic cardiomyocyte dropout with replacement fibrosis. Apoptotic loss of myocardium itself can increase haemodynamic stress through ventricular dilation and wall thinning and is therefore hypothesized to play an important role in the downward functional spiral that ultimately leads to overt heart failure.[16,29–31]

We performed TUNEL labelling on sham and TAC subjected MHC-Cre and MHC-Cre/FloxDN-MEF2 hearts, and co-stained with phalloidin and DAPI to distinguish the cardiac cell types. A representative confocal image of a merged TUNEL/phalloidin/DAPI positive cardiac myocyte is shown (*Figure 4A*). A very low incidence of TUNEL-positive cardiac myocytes was detected in the sham-operated experimental groups, a slight increase was visible in TAC MHC-Cre hearts, and a substantially higher incidence in TAC MHC-Cre/FloxDN-MEF2 hearts (*Figure 4B*). In line with these findings, detection of endogenous levels of the large fragment (89 kDa) of nuclear poly (ADP-ribose) polymerase (PARP) produced by apoptotic caspase cleavage, demonstrated increased cleaved PARP following pressure overload in

MHC-Cre mice, and more pronounced cleaved PARP levels in pressure overloaded MHC-Cre/FloxDN-MEF2 mice (*Figure 4C* and *D*). In summary, these data indicate that MHC-Cre/FloxDN-MEF2 mice display excessive production of ROS and oxidative stress-induced myocardial apoptosis following biomechanical stress.

Discussion

Previous work has provided compelling evidence that MEF2 transcription factors are intimately involved in pathological cardiac remodelling. There is a large and convincing body of literature demonstrating that cardiac MEF2 activity is under the control of HDAC regulation at the onset of cardiac hypertrophy.[10,32] The MEF2 isoforms MEF2A and MEF2D are the primary MEF2 factors expressed in the adult heart. The most compelling evidence supporting a role for MEF2 activity in pathological cardiac hypertrophy is derived from mice harbouring a conditional MEF2D allele, which were resistant to cardiac hypertrophy, foetal gene activation, and fibrosis in response to pressure overload and chronic beta-adrenergic stimulation.[11] Counter intuitively, mice lacking MEF2A died suddenly within the first week of life and exhibited pronounced dilation of the right ventricle, myofibrillar fragmentation, activation of a foetal cardiac gene program, and a deficiency of cardiac mitochondria.[7] These combined findings suggest specific roles for MEF2 isoforms in maintaining appropriate mitochondrial content and cyto-architectural integrity in the post-natal heart. The results of the present study demonstrate an overall protective role for MEF2 transcription factors in the response of the heart to pressure overload related to their role in adapting energy metabolism in the stressed myocardium.

Progression to heart failure is associated with a decrease in the activity of mitochondrial respiratory pathways leading to diminished capacity for ATP production.[23,24] Deficiencies in the mitochondrial RC are important, since reduced capacity for energy generation leads to dysregulation of processes for cardiac pump function. Interestingly, MHC-Cre/FloxDN-MEF2 mice showed a significant decrease in ND6 expression during pressure overload compared with MHC-Cre mice. Being a subunit of the mitochondrial NADH ubiquinone oxireductase (Complex I), ND6 has been postulated to contribute in proton translocation.[33] Absence of ND6 has been shown to result in failure to assemble the Complex I membrane arm that is essential for proton translocation.[33,34] Taken together, the basal decrease in ND6 expression may affect mitochondrial homeostasis in MHC-Cre/FloxDN-MEF2 mice, making these animals predisposed to the development of cardiac decompensation.

Despite its importance, the role of ND6 in the development of cardiac failure is poorly understood and has been poorly investigated. Mutations in ND6 induce a decrease in Complex I activity and the mitochondrial respiratory rate, yet total cellular energy levels did not change in cells harbouring these mutations.[35] Although different mutations have slightly different effects on Complex I activity, it has been shown that Complex II-driven ATP generation was unaffected by the impaired Complex I activity secondary to ND6 mutations.[36] In addition, a compensatory mechanism involving elevation of Complex II activity and mtDNA content was observed in leucocytes harbouring ND6 mutations.[37] Therefore, total ATP generation is unlikely to be affected in MHC-Cre/FloxDN-MEF2 mice after pressure overload.

Although ROS are generated as by-products in the mitochondria during normal oxidative metabolism, ND6 deficiencies cause Complex I dysfunction which leads to overproduction of ROS.[38] Biochemical studies have shown that Complex I dysfunction, secondary to ND6 mutations, induces cytotoxicity that is not mediated by a reduction in oxidative phosphorylation, but by increased production of ROS.[39] In line with these findings, using a marker for free radical DNA damage, 8-OHDG, we have shown that MHC-Cre/FloxDN-MEF2 mice display more oxidative damage in the heart than MHC-Cre mice after TAC. Furthermore, it has been well documented that ROS accumulation leads to progressive cardiac muscle death, especially in pressure overload.[19] Moreover, alterations in Complex I function due to ND6 mutations render the cells more susceptible to apoptosis and sensitive to diverse apoptotic stimuli than wild-type cells.[40–42] Furthermore, cells with altered ND6 expression have increased cytochrome *c* release into the cytosol, indicating activation of the mitochondrial apoptotic machinery.[43] In line with these findings, myocardium from our pressure overloaded MHC-Cre/FloxDN-MEF2 mice displayed exaggerated TUNEL positive staining *in vivo*. These data are a straight-forward explanation for the worsened cardiac function in MHC-Cre/FloxDN-MEF2 mice after biomechanical stress.

The results of this study are in seeming contrast with our previous report, which showed that reduced MEF2 transcriptional activity in calcineurin transgenic mice resulted in attenuation of cardiac dilation.[12] Biomechanical stress, however, triggers the release of a plethora of growth factors and hormones, resulting in the activation of a number of intracellular signalling cascades besides calcineurin signalling.[1,2] At least three signalling pathways besides calcineurin can impinge upon MEF2 factors, including p38 MAPK, diverse forms of CaMK, and certain forms of PKC.[1,2,10,32] Accordingly, the nature and number of cardiac MEF2 target genes downstream of selective calcineurin activation is likely to differ considerably from those target genes activated in the setting of pressure overload. In summary, our findings suggest that the inhibition of MEF2 activity provokes accelerated adverse adaptation to pressure overload secondary to Complex I deficiencies, accelerated ROS production and enhanced susceptibility to apoptosis.

Supplementary material

Supplementary material is available at *European Journal of Heart Failure* online.

Acknowledgements

We are grateful to Martin Taube and Jeroen Korving for technical assistance.

Funding

This work was supported by grants 912-04-054, 912-04-017 and a VIDI award 917-863-72 from the Netherlands Organization for Health Research and Development (ZonMW); grants NHS2003B258

and NHS2007B167 from the Netherlands Heart Foundation; the European Union Contract No. LSHM-CT-2005-018833/EUGeneHeart; and the Fondation Leducq Transatlantic Network of Excellence program 08-CVD-03 (to L.J.D.W.).

Conflict of interest: none declared.

References

1. Heineke J, Molkentin JD. Regulation of cardiac hypertrophy by intracellular signalling pathways. *Nat Rev Mol Cell Biol* 2006;**7**:589–600.
2. Lips DJ, deWindt LJ, van Kraaij DJ, Doevendans PA. Molecular determinants of myocardial hypertrophy and failure: alternative pathways for beneficial and maladaptive hypertrophy. *Eur Heart J* 2003;**24**:883–896.
3. Black BL, Olson EN. Transcriptional control of muscle development by myocyte enhancer factor-2 (MEF2) proteins. *Annu Rev Cell Dev Biol* 1998;**14**:167–196.
4. Molkentin JD, Firulli AB, Black BL, Martin JF, Hustad CM, Copeland N, Jenkins N, Lyons G, Olson EN. MEF2B is a potent transactivator expressed in early myogenic lineages. *Mol Cell Biol* 1996;**16**:3814–3824.
5. Edmondson DG, Lyons GE, Martin JF, Olson EN. Mef2 gene expression marks the cardiac and skeletal muscle lineages during mouse embryogenesis. *Development* 1994;**120**:1251–1263.
6. Passier R, Zeng H, Frey N, Naya FJ, Nicol RL, McKinsey TA, Overbeek P, Richardson JA, Grant SR, Olson EN. CaM kinase signaling induces cardiac hypertrophy and activates the MEF2 transcription factor *in vivo*. *J Clin Invest* 2000;**105**:1395–1406.
7. Naya FJ, Black BL, Wu H, Bassel-Duby R, Richardson JA, Hill JA, Olson EN. Mitochondrial deficiency and cardiac sudden death in mice lacking the MEF2A transcription factor. *Nat Med* 2002;**8**:1303–1309.
8. Kato Y, Kravchenko VV, Tapping RI, Han J, Ulevitch RJ, Lee JD. BMK1/ERK5 regulates serum-induced early gene expression through transcription factor MEF2C. *Embo J* 1997;**16**:7054–7066.
9. Marinissen MJ, Chiariello M, Pallante M, Gutkind JS. A network of mitogen-activated protein kinases links G protein-coupled receptors to the c-jun promoter: a role for c-Jun NH2-terminal kinase, p38s, and extracellular signal-regulated kinase 5. *Mol Cell Biol* 1999;**19**:4289–4301.
10. Zhang CL, McKinsey TA, Chang S, Antos CL, Hill JA, Olson EN. Class II histone deacetylases act as signal-responsive repressors of cardiac hypertrophy. *Cell* 2002;**110**:479–488.
11. Kim Y, Phan D, van Rooij E, Wang DZ, McAnally J, Qi X, Richardson JA, Hill JA, Bassel-Duby R, Olson EN. The MEF2D transcription factor mediates stress-dependent cardiac remodeling in mice. *J Clin Invest* 2008;**118**:124–132.
12. van Oort RJ, van Rooij E, Bourajjaj M, Schimmel J, Jansen MA, van der Nagel R, Doevendans PA, Schneider MD, van Echteld CJ, De Windt LJ. MEF2 activates a genetic program promoting chamber dilation and contractile dysfunction in calcineurin-induced heart failure. *Circulation* 2006;**114**:298–308.
13. Xu J, Gong NL, Bodi I, Aronow BJ, Backx PH, Molkentin JD. Myocyte enhancer factors 2A and 2C induce dilated cardiomyopathy in transgenic mice. *J Biol Chem* 2006;**281**:9152–9162.
14. Agah R, Frenkel PA, French BA, Michael LH, Overbeek PA, Schneider MD. Gene recombination in postmitotic cells. Targeted expression of Cre recombinase provokes cardiac-restricted, site-specific rearrangement in adult ventricular muscle *in vivo*. *J Clin Invest* 1997;**100**:169–179.
15. Bourajjaj M, Armand AS, da Costa Martins PA, Weijts B, van der Nagel R, Heeneman S, Wehrens XH, De Windt LJ. NFATc2 is a necessary mediator of calcineurin-dependent cardiac hypertrophy and heart failure. *J Biol Chem* 2008;**283**:22295–22303.
16. van Empel VP, Bertrand AT, van der Nagel R, Kostin S, Doevendans PA, Crijns HJ, de Wit E, Sluiter W, Ackerman SL, De Windt LJ. Downregulation of apoptosis-inducing factor in harlequin mutant mice sensitizes the myocardium to oxidative stress-related cell death and pressure overload-induced decompensation. *Circ Res* 2005;**96**:e92–e101.
17. Rockman HA, Ross RS, Harris AN, Knowlton KU, Steinhelper ME, Field LJ, Ross J Jr, Chien KR. Segregation of atrial-specific and inducible expression of an atrial natriuretic factor transgene in an *in vivo* murine model of cardiac hypertrophy. *Proc Natl Acad Sci USA* 1991;**88**:8277–8281.
18. Baurand A, Zelarayan L, Betney R, Gehrke C, Dunger S, Noack C, Busjahn A, Huelsken J, Taketo MM, Birchmeier W, Dietz R, Bergmann MW. *Circ Res* 2007;**100**:1353–1362.
19. van Empel VP, Bertrand AT, van Oort RJ, van der Nagel R, Engelen M, van Rijen HV, Doevendans PA, Crijns HJ, Ackerman SL, Sluiter W, De Windt LJ. EUK-8, a superoxide dismutase and catalase mimetic, reduces cardiac oxidative stress and ameliorates pressure overload-induced heart failure in the harlequin mouse mutant. *J Am Coll Cardiol* 2006;**48**:824–832.
20. van Rooij E, Doevendans PA, de Theije CC, Babiker FA, Molkentin JD, de Windt LJ. Requirement of nuclear factor of activated T-cells in calcineurin-mediated cardiomyocyte hypertrophy. *J Biol Chem* 2002;**277**:48617–48626.
21. Booth FW, Thomason DB. Molecular and cellular adaptation of muscle in response to exercise: perspectives of various models. *Physiol Rev* 1991;**71**:541–585.
22. Kelly DP, Strauss AW. Inherited cardiomyopathies. *N Engl J Med* 1994;**330**:913–919.
23. Ingwall JS, Weiss RG. Is the failing heart energy starved? On using chemical energy to support cardiac function. *Circ Res* 2004;**95**:135–145.
24. Arany Z, He H, Lin J, Hoyer K, Handschin C, Toka O, Ahmad F, Matsui T, Chin S, Wu PH, RybkinII, Shelton JM, Manieri M, Cinti S, Schoen FJ, Bassel-Duby R, Rosenzweig A, Ingwall JS, Spiegelman BM. *Cell Metab* 2005;**1**:259–271.
25. Arany Z, Novikov M, Chin S, Ma Y, Rosenzweig A, Spiegelman BM. Transverse aortic constriction leads to accelerated heart failure in mice lacking PPAR-gamma coactivator 1alpha. *Proc Natl Acad Sci USA* 2006;**103**:10086–10091.
26. Czubryt MP, Olson EN. Balancing contractility and energy production: the role of myocyte enhancer factor 2 (MEF2) in cardiac hypertrophy. *Recent Prog Horm Res* 2004;**59**:105–124.
27. Ishikawa K, Takenaga K, Akimoto M, Koshikawa N, Yamaguchi A, Imanishi H, Nakada K, Honma Y, Hayashi J. ROS-generating mitochondrial DNA mutations can regulate tumor cell metastasis. *Science* 2008;**320**:661–664.
28. Lorell BH, Carabello BA. Left ventricular hypertrophy: pathogenesis, detection, and prognosis. *Circulation* 2000;**102**:470–479.
29. Hirota H, Chen J, Betz UA, Rajewsky K, Gu Y, Ross J Jr, Müller W, Chien KR. Loss of a gp130 cardiac muscle cell survival pathway is a critical event in the onset of heart failure during biomechanical stress. *Cell* 1999;**97**:189–198.
30. Zhang D, Gaussin V, Taffet GE, Belaguli NS, Yamada M, Schwartz RJ, Michael LH, Overbeek PA, Schneider MD. TAK1 is activated in the myocardium after pressure overload and is sufficient to provoke heart failure in transgenic mice. *Nat Med* 2000;**6**:556–563.
31. Sadoshima J, Montagne O, Wang Q, Yang G, Warden J, Liu J, Takagi G, Karoor V, Hong C, Johnson GL, Vatner DE, Vatner SF. The MEKK1-JNK pathway plays a protective role in pressure overload but does not mediate cardiac hypertrophy. *J Clin Invest* 2002;**110**:271–279.
32. Chang S, McKinsey TA, Zhang CL, Richardson JA, Hill JA, Olson EN. Histone deacetylases 5 and 9 govern responsiveness of the heart to a subset of stress signals and play redundant roles in heart development. *Mol Cell Biol* 2004;**24**:8467–8476.
33. Bai Y, Attardi G. The mtDNA-encoded ND6 subunit of mitochondrial NADH dehydrogenase is essential for the assembly of the membrane arm and the respiratory function of the enzyme. *EMBO J* 1998;**17**:4848–4858.
34. Chomyn A. Mitochondrial genetic control of assembly and function of complex I in mammalian cells. *J Bioenerg Biomembr* 2001;**33**:251–257.
35. Yen MY, Lee JF, Liu JH, Wei YH. Energy charge is not decreased in lymphocytes of patients with Leber's hereditary optic neuropathy with the 11,778 mutation. *J Neuroophthalmol* 1998;**18**:84–85.
36. Baracca A, Solaini G, Sgarbi G, Lenaz G, Baruzzi A, Schapira AH, Martinuzzi A, Carelli V. Severe impairment of complex I-driven adenosine triphosphate synthesis in leber hereditary optic neuropathy cybrids. *Arch Neurol* 2005;**62**:730–736.
37. Yen MY, Lee HC, Liu JH, Wei YH. Compensatory elevation of complex II activity in Leber's hereditary optic neuropathy. *Br J Ophthalmol* 1996;**80**:78–81.
38. Robinson BH. Human complex I deficiency: clinical spectrum and involvement of oxygen free radicals in the pathogenicity of the defect. *Biochim Biophys Acta* 1998;**1364**:271–286.
39. Barrientos A, Moraes CT. Titrating the effects of mitochondrial complex I impairment in the cell physiology. *J Biol Chem* 1999;**274**:16188–16197.
40. Battisti C, Formichi P, Cardaioli E, Bianchi S, Mangiavacchi P, Tripodi SA, Tosi P, Federico A. Cell response to oxidative stress induced apoptosis in patients with Leber's hereditary optic neuropathy. *J Neurol Neurosurg Psychiatry* 2004;**75**:1731–1736.
41. Danielson SR, Wong A, Carelli V, Martinuzzi A, Schapira AH, Cortopassi GA. Cells bearing mutations causing Leber's hereditary optic neuropathy are sensitized to Fas-Induced apoptosis. *J Biol Chem* 2002;**277**:5810–5815.
42. Zanna C, Ghelli A, Porcelli AM, Martinuzzi A, Carelli V, Rugolo M. Caspase-independent death of Leber's hereditary optic neuropathy cybrids is driven by energetic failure and mediated by AIF and Endonuclease G. *Apoptosis* 2005;**10**:997–1007.
43. Ghelli A, Zanna C, Porcelli AM, Schapira AH, Martinuzzi A, Carelli V, Rugolo M. Leber's hereditary optic neuropathy (LHON) pathogenic mutations induce mitochondrial-dependent apoptotic death in transmitochondrial cells incubated with galactose medium. *J Biol Chem* 2003;**278**:4145–4150.